Available online at www.sciencedirect.com

SciVerse ScienceDirect

Ceramics International 39 (2013) 7143–7148

CERAMICS INTERNATIONAL

www.elsevier.com/locate/ceramint

Fabrication and photocatalytic activity of electrospun nylon-6 nanofibers containing tourmaline and titanium dioxide nanoparticles

Seung-Ji Kang[a,1], Leonard D. Tijing[a,b,*,1], Bo-sang Hwang[a], Zhe Jiang[c], Hak Yong Kim[d,e], Cheol Sang Kim[a,c,*]

[a]*Division of Mechanical Design Engineering, Chonbuk National University, Jeonju, Jeonbuk 561-756, Republic of Korea*
[b]*Department of Mechanical Engineering, College of Engineering and Design, Silliman University, Dumaguete City, Negros Oriental 6200, Philippines*
[c]*Department of Bionanosystem Engineering, Graduate School, Chonbuk National University, Jeonju, Jeonbuk 561-756, Republic of Korea*
[d]*Department of Organic Materials and Fiber Engineering, Chonbuk National University, Jeonju, Jeonbuk 561-756, Republic of Korea*
[e]*Center for Healthcare Technology Development, Chonbuk National University, Jeonju, Jeonbuk 561-756, Republic of Korea*

Received 18 January 2013; received in revised form 18 February 2013; accepted 18 February 2013
Available online 14 March 2013

Abstract

In this paper, we report the effect of the incorporation of titanium dioxide (TiO_2) nanoparticles (NPs) on the photocatalytic properties of a tourmaline NP/nylon-6 composite mat prepared by one-step electrospinning process. Several characterization techniques were utilized to check the successful incorporation of NPs in/on the nanofibers. Both TiO_2 and tourmaline NPs were confirmed to be incorporated on the surface of the nylon-6 nanofibers or fully embedded in the fibers through SEM and TEM observations. The fiber diameter showed increasing size trend in the order of nylon-6 < tourmaline/nylon-6 < TiO_2-tourmaline/nylon-6. The incorporation of both TiO_2 and tourmaline NPS on/in nylon-6 nanofibers has resulted to increased photocatalytic degradation of organic pollutant. The successful immobilization on nylon-6 nanofibers through simple electrospinning of tourmaline possessing unique properties, and photocatalytic TiO_2 showed synergistic effect in the degradation of organic pollutants, which could have potential application in water treatment applications.

Keywords: D. TiO_2; Electrospinning; Photocatalytic; Tourmaline; Nylon-6

1. Introduction

Among the current technologies, electrospinning of nanofibers presents itself as a simple and effective method in fabricating nanofibrous materials decorated with or containing nanoparticles [1–4]. Electrospun nanofibers have very large surface areas providing more reactive sites and small pore sizes, which can then be utilized in different applications such as in water and air filtration, textiles, and in biomedical engineering [5,6]. There are many filler materials available to functionalize nanofibrous mats, and most of the reports include the use of nanoparticles (NPs) such as Ag, TiO_2, zinc oxide, carbon nanotubes, grapheme, alumina, silica, etc. Only few studies have incorporated tourmaline nanoparticles to impart functionalities on a nanofibrous mat. In our previous study, we reported an increase in mechanical properties and wettability of polyurethane (PU) nanofibers when tourmaline nanoparticles were incorporated [7]. Synergistic effects in killing bacteria was also realized when tourmaline nanoparticles were exposed in high frequency electric fields [8]. Tourmaline (TM) is a type of complex borosilicate material belonging to a trigonal space group [9]. Its general formula can be expressed as $XY_3Z_6[T_6O_{18}][BO_3]_3V_3W$, where X = Na, K, Ca, (vacancy); Y = Li, Mg, Fe^{2+}, Mn^{2+}, Al, Cr^{3+}, V^{3+}, Fe^{3+}, Ti; Z = Al, Fe^{3+}, Cr^{3+}, V^{3+}, Mg; T = Si, Al; V = OH, O; W = OH, F, O [10,11]. Tourmaline possesses spontaneous surface electric fields,

*Corresponding authors at: Division of Mechanical Design Engineering, Chonbuk National University, Jeonju, Jeonbuk 561-756, Republic of Korea. Tel.: +82 63 270 4284; fax: +82 63 270 2460.
E-mail addresses: ltijing@jbnu.ac.kr, ltijing@gmail.com (L.D. Tijing), chskim@jbnu.ac.kr (C.S. Kim).
[1]These authors contributed equally to this work.

0272-8842/$ - see front matter © 2013 Elsevier Ltd and Techna Group S.r.l. All rights reserved.
http://dx.doi.org/10.1016/j.ceramint.2013.02.057

and it has been utilized in different applications such as heavy metal absorption [9,12], bacterial inactivation [13], and decomposition of waste water contaminants [14]. We also paired tourmaline NPs with Ag NPs on PU mat by electrospinning and UV photoreduction, and found better bacterial inactivation compared to tourmaline/PU composite mat and PU mat only.

In this study, we impart photocatalytic properties on a tourmaline/nylon-6 composite mat by incorporating TiO_2 nanoparticles. Titanium dioxide (TiO_2) is one of the most widely used photocatalysts because it is cheap and easily available, non-toxic, and has relatively high chemical stability [15,16]. TiO_2 is useful for UV solar absorption and has some important photonic applications too [17]. However, TiO_2 possesses wide band gap (3.2 eV), which can only absorb a UV fraction of solar light (3–5%), making it not very efficient in solar-assisted photocatalysis [18]. Noble metal deposition, non-metal doping and semiconductor coupling are some of the methods used to enhance the photocatalytic performance of TiO_2 [19]. The unique properties of tourmaline make it desirable for the enhancement of TiO_2 performance in photocatalysis. Yeredla and Xu [20] reported that the surface electric fields of tourmaline can enhance the e^-–h^+ pairs separation of TiO_2 and improve the photosplitting of water. They conducted their experiments using TiO_2-tourmaline composite in powder form. Nylon-6 is one of the most used engineering polymers because of its excellent mechanical and thermal properties, easy to process, and good compatibility with other materials.

Here, we immobilized both TiO_2 and tourmaline NPs on/in nylon-6 nanofibers via a simple electrospinning process. Our objective in this study was to determine the synergistic effect of the incorporation of TiO_2 and tourmaline NPs on the physical, and photocatalytic properties of the electrospun composite nanofibers.

2. Experimental

Neat nylon-6 (KN20 grade, Mw=35,000, Kolon, Korea) solution was prepared by dissolving 20 wt% nylon-6 pellets in 4:1 solvent mixture of formic acid/acetic acid. To prepare tourmaline (TM)/nylon-6 or titanium dioxide-tourmaline/nylon-6 (TiO_2-tourmaline/nylon-6) solution, 3 wt% TM (ball-milled, UBS) or a mixture of 3 wt% TM and 3 wt% TiO_2 (TiO_2, anatase, d=500 nm) NPs in a given amount of formic acid/acetic acid solution was first sonicated in a homogenizer at 10,000 rpm for at least 30 min and then added to the neat nylon-6 solution and stirred by magnetic stirring overnight. Note that the wt% of TM and TiO_2 were based on the weight of nylon-6. The prepared solutions were then directly electrospun onto a flat metallic substrate at an applied voltage of 20 kV, a tip-to-collector distance of 15 cm, and a solution feed rate of 0.3 ml/h. The spinneret with an inner diameter of 0.51 mm makes a translational oscillatory motion perpendicular to the flat substrate driven by a step motor with an oscillation distance of about 20 cm. After electrospinning, the collected nanofibrous mat was dried in an oven at 60 °C for at least 48 h. The prepared electrospun mat samples are named as S0, S1, and S2 corresponding to neat nylon-6, TM/nylon-6 and TiO_2-TM/nylon-6, respectively.

Morphological characterizations were carried out by field emission scanning electron microscopy (FESEM, Hitachi S-4800, Japan) and transmission electron microscopy (TEM, H-7650, Hitachi, Japan). The samples for FESEM were coated with platinum using a Pt coater (K575x, Emitech) and examined at an accelerating voltage of 15 kV. The TEM samples for nanofibers were prepared by electrospinning directly on a copper grid mesh coated with carbon and formar for 15 s. The distribution of fiber sizes was determined using an image processing software (ImageJ, NIH, USA), checking the diameters of at least 100 fibers and the average was calculated. Water contact angle measurements were carried out using GBX, Digidrop (France) water contact angle meter. Deionized water with a drop diameter of 6 μm was automatically dropped onto the mat. The FTIR spectra of the samples were measured using a Paragon 1000 Spectrometer (Perkin Elmer, USA) in the range of 400–4000 cm^{-1} with a signal resolution of 1 cm^{-1} and a minimum of 16 scans. X-ray powder diffraction (XRD) analysis was carried out by a Rigaku X-ray diffractometer (Cu Kα, λ=1.54059 Å) over Bragg angles ranging from 20° to 80°.

The photocatalytic activity of the composite mats was assessed by the degradation of methylene blue (MB). Here, photocatalytic reactions were carried out in Petri dishes (d=55 mm, h=15 mm). A 10-ppm dye concentration (dye volume=10 ml) was reacted with the nanofibrous mat samples (size=30 mm × 30 mm) in the Petri dish under UV light irradiation (320–500 nm, Omnicure). At specific time intervals, samples of the reacted dye solution were taken out and were subjected to UV–vis spectroscopy measuring their absorbance at 663 nm.

3. Results and discussion

Fig. 1 shows the SEM images and the corresponding EDS spectra and contact angles of the prepared samples. The neat nylon-6 sample showed uniform, smooth and beadless fibers with an average diameter of 120 ± 24 nm (Fig. 1a). The addition of 3 wt% TM NPs (Fig. 1b) to nylon-6 solution resulted to thicker nanofibers (d=130 ± 25 nm) and further addition of TiO_2 NPs (Fig. 1c) increased the fiber diameter to 153 ± 41 nm. The increase in fiber diameter could be attributed to the increase in the viscosity of the electrospinning solution when nanopartiles were incorporated as also observed in other studies. Tourmaline and TiO_2 NPs can be clearly observed to be deposited on/in the nanofibers. Some beads were observed to form on the fiber surfaces of S3 (TiO_2–TM/nylon-6), which could be due to the increased viscosity of S3 solution. Increased soluton viscosity requires more energy to overcome the surface tension for electrospinning,

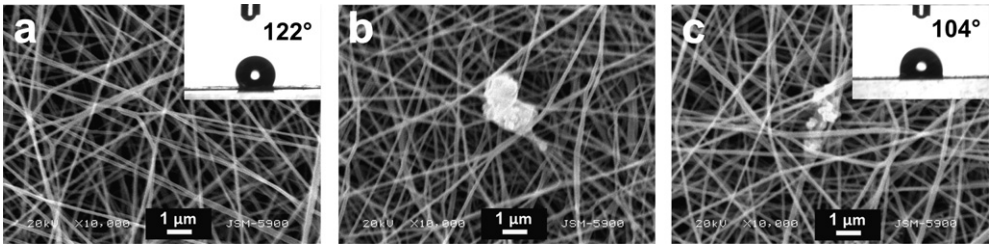

Fig. 1. SEM images of electrospun mats from (a) neat nylon-6, (b) tourmaline/nylon-6, and (c) TiO_2-tourmaline/nylon-6. The insets show the respective contact angle measurements.

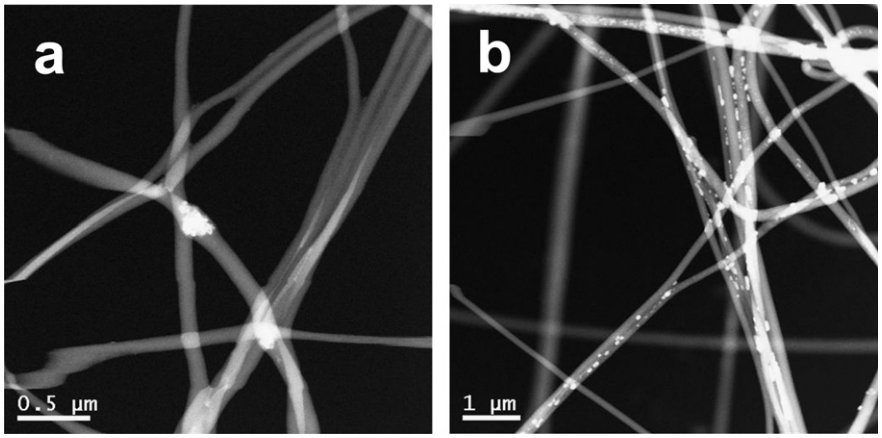

Fig. 2. TEM images of electrospun nanofibrous mats from (a) tourmaline/nylon-6, and (b) TiO_2-tourmaline/nylon-6.

thus resulting to some bead formation and thicker fibers [21]. The EDS spectra (not shown) also confirmed the presence of both tourmaline and TiO_2 NPs on the nanofibers. Contact angle is a quantitative measure of the wettability of a surface [22,23]. The wettability of the samples was observed to be more hydrophilic when nanoparticles where incorporated from a contact angle of 122° for the neat nylon-6 mat (Fig. 1a inset), to 110° and 104° (Fig. 1c inset) for the TM/nylon-6 and TiO_2-TM/nylon-6 mats, respectively. The increase in hydrophilicity was expected since TM and TiO_2 NPs are hydrophilic in nature. The better hydrophilic behavior of the nanofibrous composites increases their antifouling property, since it was reported that hydrophilic surface has less tendency to fouling compared to hydrophobic surface especially for water filtration application [24]. Fig. 2 shows the TEM images of the composite mats. Tourmaline (Fig. 2a) and TM–TiO_2 (Fig. 2b) nanoparticles are observed to be embedded in and on the surface of the nanofibers and were distributed uniformly. The TEM line-EDS in Fig. 3 confirms the presence of both tourmaline and TiO_2 NPs along the fiber. Elements of tourmaline such as potassium, sodium, silicon and chlorine were clearly obtained as well as titanium, signifying the presence of both NPs.

The XRD spectra of the samples are shown in Fig. 4. The peak at $2\theta = 21.3°$ in Fig. 4a signifies the γ-phase crystalline peak (200) of nylon-6 [25]. The pattern of Tm/nylon-6 composite showed an additional peak at $2\theta = 26.3°$, a characteristic peak of the present tourmaline. The TiO_2–TM/nylon-6 composite mat also had same crystalline characteristic peaks analogous with the characteristic peaks of nylon-6 and tourmaline, and additional anatase TiO_2 peaks at $2\theta = 25.2°$ and 37.6° [26]. The XRD results further proves the successful incorporation and uniform distribution of nanoparticles in/on the nylon-6 mat by simple electrospinning. To observe whether there was interaction between nylon-6 and nanoparticles, we further evaluated the mats through FT-IR. Fig. 5 shows the infrared spectra of the present samples. All samples showed the characteristic peaks of nylon-6 as reported in literature [25]. The bands at 3300 cm^{-1}, 3098 cm^{-1}, 2931 cm^{-1}, 2865 cm^{-1}, 2208 cm^{-1}, 1647 cm^{-1}, 1560 cm^{-1}, and 719 cm^{-1} can be assigned to hydrogen-bonded N–H stretching, NH Fermi resonance, CH_2 asymmetric stretching, CH_2 symmetric stretching, C≡N stretching, amide I, amide II, and amide V(γ), respectively [25]. However, for the TM/nylon-6 and TiO_2-TM/nylon-6 composite mats, a slight shift to the right was observed at 2208 cm^{-1} indicating a possible interaction between nylon-6 and the nanoparticles.

The photocatalytic activity of the present samples were evaluated by degrading organic pollutant methylene blue (MB) under UV-light irradiation. As shown in Fig. 6, insignificant degradation of MB occured when only neat nylon-6 was irradiated with UV. In the presence of tourmaline NPs on/in nylon-6 nanofibers, a much better photocatalytic degradation compared to nylon-6 was observed. Faster degradation rate was obtained when both TiO_2 and tourmaline nanoparticles were incorporated

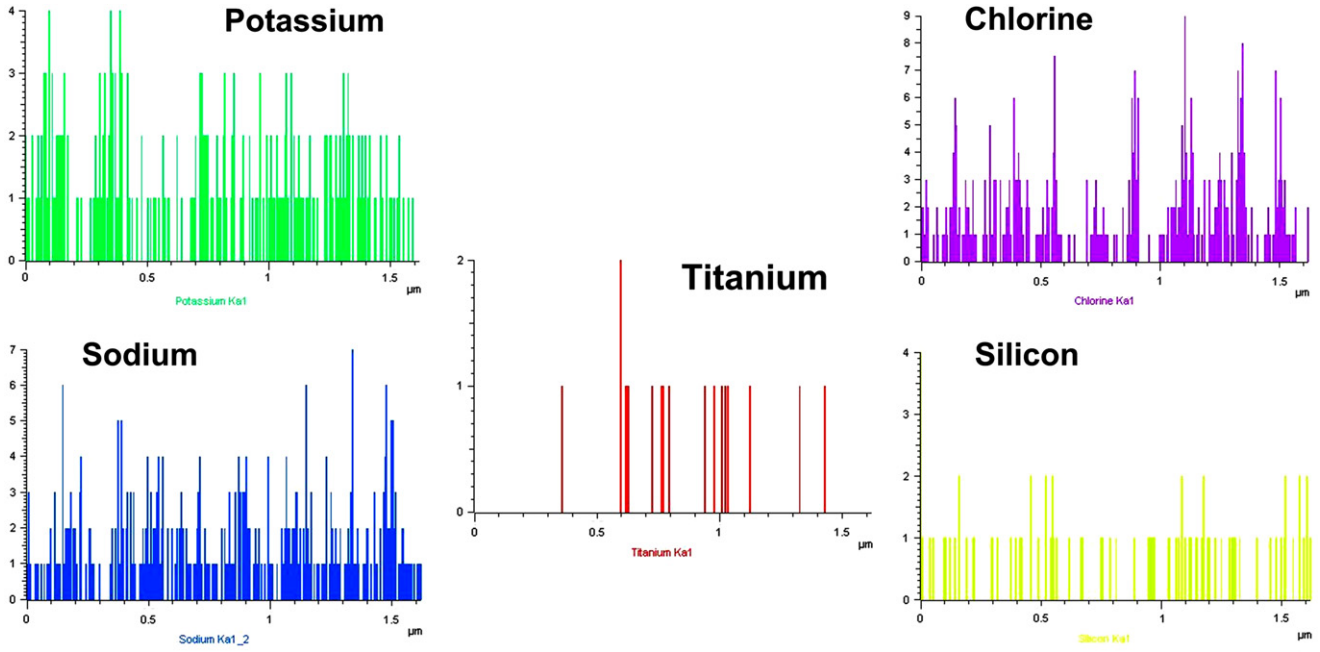

Fig. 3. TEM line-EDX of TiO_2-tourmaline/nylon-6 nanofibers.

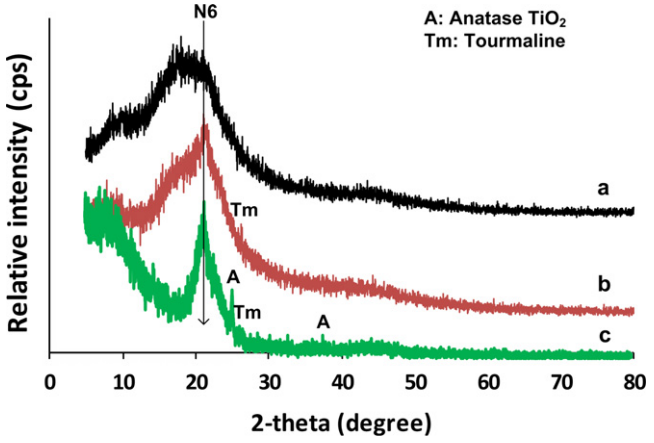

Fig. 4. XRD spectra of electrospun mats from (a) neat nylon-6, (b) tourmaline/nylon-6, and (c) TiO_2-tourmaline/nylon-6.

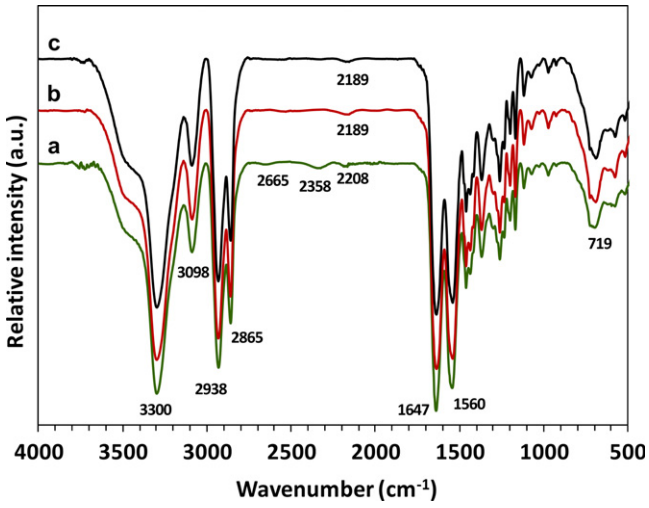

Fig. 5. FT-IR spectra of electrospun mats from (a) neat nylon-6, (b) tourmaline/nylon-6, and (c) TiO_2-tourmaline/nylon-6.

on/in the nylon-6 electrospun mat. After 180 min of UV irradiation, the MB degradation performance was in the order S3 > S2 > S1. For S3, tourmaline NP serves as an electron acceptor of the photogenerated electrons from anatase TiO_2, which effectively suppress the recombination of e^-–h^+ pairs, and leaves more photogenerated holes to form reactive species that can facilitate the degradation of MB pollutant [27]. Yeredla and Xu [20] reported an improved photosplitting of water when tourmaline was integrated with Degussa P25 titania. The inherent surface electric fields of tourmaline could have possibly caused the reduction of barrier potential for the migration of charge carriers to the surface of TiO_2 by reducing the band bending in the space charge layer and increasing the chemical potential of the electrons in TiO_2. This leads to spatially separated oxidation and reduction reactions, with a reduced oxidation potential for the photogenerated holes [20].

4. Conclusions

In this report, we have successfully immobilized both TiO_2 and tourmaline nanoparticles in/on nylon-6 nanofibers by simple electrospinning process. Various techniques were utilized to characterize the fabricated composite nanofibers. The incorporation of nanoparticles has resulted to bigger fiber diameters with TiO_2-tourmaline/nylon-6 nanofibers showing the largest average fiber diameter. This is attributed to the increase in viscosity of the composite solution. SEM

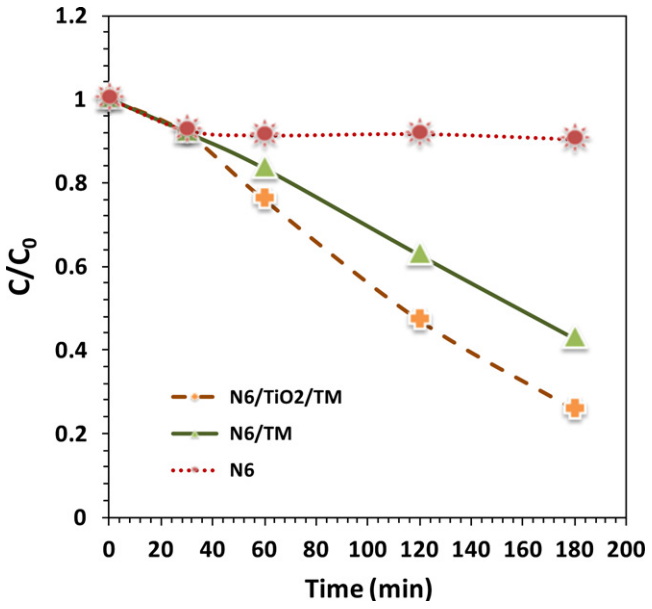

Fig. 6. Photocatalytic degradation of methylene blue utilizing different electrospun mat samples of (a) neat nylon-6, (b) tourmaline/nylon-6, and (c) TiO_2-tourmaline/nylon-6.

and TEM images clearly showed embedded nanoparticles on the surface or at the internal layer of the nylon-6 nanofibers. TEM-EDS and XRD have confirmed the presence of TiO_2 and tourmaline NPs in the composite nanofibers. TiO_2-tourmaline/nylon-6 mat under UV light showed the highest photocatalytic performance among the present samples. The incorporation of both TiO_2 and tourmaline NPs in/on nylon-6 nanofibers showed synergistic effects on improving the photocatalytic degradation of methylene blue, and could find potential application in water treatment.

Acknowledgments

This research was supported by a grant from the Basic Science Research Program through the National Research Foundation of Korea (NRF) funded by the Ministry of Education, Science and Technology (MEST) (Project nos. 2012-0001611 and 2012-013341), and also by a grant from MEST and NRF through the Human Resource Training Project for Regional Innovation (Project no. 2012H1B8A2025931). We also would like to thank KBSI-Jeonju (Korea) for taking high-quality TEM images.

References

[1] S. Nataraj, K. Yang, T. Aminabhavi, Polyacrylonitrile-based nanofibers-A state-of-the-art review, Progress in Polymer Science 37 (2012) 487–513.

[2] N.A.M. Barakat, M.A. Kanjwal, F.A. Sheikh, H.Y. Kim, Spider-net within the N6, PVA and PU electrospun nanofiber mats using salt addition: Novel strategy in the electrospinning process, Polymer 50 (2009) 4389–4396.

[3] J.S. Xie, Q.S. Wu, D.F. Zhao, Electrospinning synthesis of $ZnFe_2O_4$/Fe_3O_4/Ag nanoparticle-loaded mesoporous carbon fibers with magnetic and photocatalytic properties, Carbon 50 (2012) 800–807.

[4] P.T. Zhao, J.T. Fan, Electrospun nylon 6 fibrous membrane coated with rice-like TiO_2 nanoparticles by an ultrasonic-assistance method, Journal of Membrane Science 355 (2010) 91–97.

[5] S. Lee, Multifunctionality of layered fabric systems based on electrospun polyurethane/zinc oxide nanocomposite fibers, Journal of Applied Polymer Science 114 (2009) 3652–3658.

[6] M. Botes, T.E. Cloete, The potential of nanofibers and nanobiocides in water purification, Critical Reviews in Microbiology 36 (2010) 68–81.

[7] L.D. Tijing, M.T.G. Ruelo, A. Amarjargal, H.R. Pant, C.H. Park, D.W. Kim, C.S. Kim, Antibacterial and superhydrophilic electrospun polyurethane nanocomposite fibers containing tourmaline nanoparticles, Chemical Engineering Journal 197 (2012) 41–48.

[8] A. Amarjargal, L.D. Tijing, M.T.G. Ruelo, C.-H. Park, H.R. Pant, F.P. Vista IV, D.H. Lee, C.S. Kim, Inactivation of bacteria in batch suspension by fluidized ceramic tourmaline nanoparticles under oscillating radio frequency electric fields, Ceramics International 39 (2012) 2141–2145.

[9] Y.A. Zheng, A.Q. Wang, Removal of heavy metals using polyvinyl alcohol semi-IPN poly(acrylic acid)/tourmaline composite optimized with response surface methodology, Chemical Engineering Journal 162 (2010) 186–193.

[10] L.P. Ogorodova, L.V. Melchakova, I.A. Kiseleva, I.S. Peretyazhko, Thermodynamics of natural tourmaline-elbaite, Thermochimica Acta 419 (2004) 211–214.

[11] F. Yavuz, A.H. Gultekin, M.C. Karakaya, CLASTOUR: a computer program for classification of the minerals of the tourmaline group, Computers and Geosciences (UK) 28 (2002) 1017–1036.

[12] K. Jiang, T.H. Sun, L.N. Sun, H.B. Li, Adsorption characteristics of copper, lead, zinc and cadmium ions by tourmaline, Journal of Environmental Sciences (China) 18 (2006) 1221–1225.

[13] S. Qiu, F. Ma, Y. Wo, S.W. Xu, Study on the biological effect of tourmaline on the cell membrane of *E. coli*, Surface and Interface Analysis 43 (2011) 1069–1073.

[14] S.H. Song, M. Kang, Decomposition of 2-chlorophenol using a tourmaline-photocatalytic system, Journal of Industrial and Engineering Chemistry 14 (2008) 785–791.

[15] Q.J. Xiang, J.G. Yu, M. Jaroniec, Synergetic effect of MoS_2 and graphene as cocatalysts for enhanced photocatalytic H-2 production activity of TiO_2 nanoparticles, Journal of the American Chemical Society 134 (2012) 6575–6578.

[16] A.L. Linsebigler, G.Q. Lu, J.T. Yates, Photocatalysis on TiO_2 surfaces—principles, mechanisms, and selected results, Chemical Reviews 95 (1995) 735–758.

[17] R. Pandiyan, V. Micheli, D. Ristic, R. Bartali, G. Pepponi, M. Barozzi, G. Gottardi, M. Ferrari, N. Laidani, Structural and near-infra red luminescence properties of Nd-doped TiO_2 films deposited by RF sputtering, Journal of Materials Chemistry 22 (2012) 22424–22432.

[18] Y.S. Li, F.L. Jiang, Q. Xiao, R. Li, K. Li, M.F. Zhang, A.Q. Zhang, S.F. Sun, Y. Liu, Enhanced photocatalytic activities of TiO_2 nanocomposites doped with water-soluble mercapto-capped CdTe quantum dots, Applied Catalysis B: Environmental 101 (2010) 118–129.

[19] H.I. Kim, J. Kim, W. Kim, W. Choi, Enhanced photocatalytic and photoelectrochemical activity in the ternary hybrid of CdS/TiO_2/WO_3 through the cascadal electron transfer, Journal of Physical Chemistry C 115 (2011) 9797–9805.

[20] R.R. Yeredla, H.F. Xu, Incorporating strong polarity minerals of tourmaline with semiconductor titania to improve the photosplitting of water, Journal of Physical Chemistry C 112 (2008) 532–539.

[21] L.D. Tijing, A. Amarjargal, Z Jiang, M.T.G. Ruelo, C.H. Park, H.R. Pant, D.W. Kim, D.H. Lee, C.S. Kim, Antibacterial tourmaline nanoparticles/polyurethane hybrid mat decorated with silver

nanoparticles prepared by electrospinning and UV photoreduction, Current Applied Physics 13 (2013) 205–210.

[22] P. Roach, N.J. Shirtcliffe, M.I. Newton, Progess in superhydrophobic surface development, Soft Matter 4 (2008) 224–240.

[23] S.A. Wang, Y.P. Li, X.L. Fei, M.D. Sun, C.Q. Zhang, Y.X. Li, Q.B. Yang, X. Hong, Preparation of a durable superhydrophobic membrane by electrospinning poly (vinylidene fluoride) (PVDF) mixed with epoxy-siloxane modified SiO_2 nanoparticles: A possible route to superhydrophobic surfaces with low water sliding angle and high water contact angle, Journal of Colloid and Interface Science 359 (2011) 380–388.

[24] L. Zou, I. Vidalis, D. Steele, A. Michelmore, S.P. Low, J.Q.J.C. Verberk, Surface hydrophilic modification of RO membranes by plasma polymerization for low organic fouling, Journal of Membrane Science 369 (2011) 420–428.

[25] K.H. Lee, K.W. Kim, A. Pesapane, H.Y. Kim, J.F. Rabolt, Polarized FT-IR study of macroscopically oriented electrospun nylon-6 nanofibers, Macromolecules 41 (2008) 1494–1498.

[26] C. Wen, Y.J. Zhu, T. Kanbara, H.Z. Zhu, C.F. Xiao, Effects of I and F codoped TiO_2 on the photocatalytic degradation of methylene blue, Desalination 249 (2009) 621–625.

[27] K.X. Li, T. Chen, L.S. Yan, Y.H. Dai, Z.M. Huang, H.Q. Guo, L.X. Jiang, X.H. Gao, J.J. Xiong, D.Y. Song, Synthesis of mesoporous graphene and tourmaline co-doped titania composites and their photocatalytic activity towards organic pollutant degradation and eutrophic water treatment, Catalysis Communications 28 (2012) 196–201.